

STRUCTURAL AND MECHANICAL RESPONSE OF ARTIFICIALLY AGED ALUMINUM ALLOY 6061

A. Ahmad, N. Afzal,¹
and M. Rafique

UDC 539.4

This work investigates the structural and mechanical changes in Al-Mg-Si (Al-6061) alloy due to its artificial aging at different temperatures and time. The Al-6061 samples were given solution heat treatment at 500°C for 2 h in a vacuum furnace. The solution treated (ST) samples were naturally aged for 20 days and then were given artificial aging heat treatment at 140, 160, 180, 200, and 220°C for 4 h. In order to find out the optimum aging time for the age hardening, another set of solution treated samples was aged at 200°C for 1, 4, and 7 h. Structural characterization revealed Mg₂Si precipitates whose size was increased with increase of aging temperature. The surface morphology results showed precipitate particles on the alloy surface that were increased at 200°C. The maximum engineering yield stress and ultimate tensile stress were found to be 291 and 319 MPa for the sample aged at 200°C, whereas the percentage elongation at this temperature was reduced to 55%, as compared to the solution treated sample. Similarly, the maximum value of Vickers hardness (92 HV) was noticed at 200°C, whereas with further increase of the aging temperature, the hardness was decreased. The hardness and tensile test measurements of Al-6061 aged at 200°C for different duration revealed their maximum values at 4 h aging time. As the aging time was further increased to 7 h, both the hardness and strength of the material were decreased. The increase of the Al-6061 strength and hardness after aging heat treatment was attributed to an increase in the resistance offered by the Mg₂Si precipitates to the dislocation motion during deformation that became more effective as the aging time was increased up to 4 h.

Keywords: aging, Al-Mg-Si alloy, precipitates, engineering stress, elongation, hardness.

Introduction. Al-Mg-Si (Al-6061) is an alloy whose strength can be increased by heat treatment. The Al-6061 is often used in the automotive body parts as substitution for steel to reduce the weight of vehicle and the energy consumption [1, 2]. Practically, the Al-6061 alloy is naturally aged between the annealing and paint baking temperature, however, the natural aging can reduce the strength of the alloy and it has negative impact on its hardness [3]. Therefore, artificial aging of this alloy is necessary to increase its strength which can be used for the multipurpose such as aerospace, automotive, marine industry and many other engineering applications [4, 5]. Therefore, the age hardening study has been a prime and interesting topic of research. In the artificial aging, an alloy is initially given solution heat treatment (SHT) up to a certain temperature (near to its melting point) and then it is rapidly cooled to room temperature. During the SHT process, the solutes in the alloy are completely dissolved and form a single-phase supersaturated solution (SSSS) [6–10]. The SSSS transforms into clusters [11] of Mg and Si immediately and then with the passage of time, the clusters transform into GP Zones (arrays of atoms) that further change into different types of precipitates. The β'' and β' are the semi-coherent metastable precipitates of Mg and

Center for Advanced Studies in Physics, GC University, Lahore, Pakistan (¹Naveed.phys@gmail.com).
Translated from Problemy Prochnosti, No. 3, pp. 129 – 137, May – June, 2021. Original article submitted January 23, 2020.

Si. These precipitates transform into the stable and incoherent MgSi_2 (β) precipitates, which contribute to the hardening mechanism [12].

Several studies have been conducted to study precipitation sequence in Al-6061 alloy after its artificial aging under different conditions [13]. Tan et al. [14] investigated the precipitation hardening behavior of aluminum alloy 6061 (AA6061) at different aging temperatures ranging from 175 to 420°C for different durations. The authors found that the Al-6061 shows optimum strength and hardness at 185°C with 2 to 6 h aging time. The hardness and strength of the alloy decreases with further increase of the aging temperature. Naronikar et al. [15] studied the effect of artificial aging on the strength and percentage elongation of AA6061. The strength and percentage elongation of the alloy was noticed to be maximum after aging at 120°C for 6 and 2 h, respectively. The stepped aging of the sample at 300°C significantly increased the percentage elongation of the alloy; however, the alloy strength was decreased.

In the age hardening studies of Al-6061, the time-temperature combination plays an important role in controlling the strength and ductility of the alloy. Therefore efforts are in progress to find out a suitable combination of aging temperature and time. In this work, both aging time and temperatures were varied to obtain the optimum strength, hardness and ductility of the Al-6061 alloy.

1. Experimental Work. The Al-Mg-Si (Al-6061) was obtained from the Alfa Aesar (USA). The chemical composition of Al-Mg-Si alloy was 1 wt.% Mg, 0.6 wt.% Si, 0.27 wt.% copper, 0.2 wt.% Cr, and balance Al. Two types of samples were prepared in this work. The circular samples were prepared for the structural, morphological and hardness studies, whereas for the tensile testing, the rod-shaped samples of length 5 × 5 cm were used. The circular shaped Al-6061 samples were grinded and polished. The grinding of the samples was made by using emery papers of grits, 1000, 1500, 2000, and 3000 followed by their polishing using diamond paste up to 3 μm . The samples of Al-6061 were given solution heat treatment (ST) at 500°C under vacuum for two hours and then were rapidly quenched to room temperature in clean water. The ST samples were artificially aged at 140, 160, 180, 200, and 220°C for four hours and afterwards these were rapidly cooled in clean water. The artificially aged samples were then kept at room temperature for about 20 days before their characterizations. The structural results of the aged samples were obtained through X-ray diffractometer (Philips Panalytical) operated with Cu-k alpha radiations ($\lambda = 0.15406 \text{ nm}$) with voltage of 40 keV and 20 mA current. The range of 2θ was from 20 to 80° with the step size of 0.15°. The surface morphology of solution treated and the aged samples was studied using scanning electron microscope. The mechanical testing of the samples was performed using Vickers hardness tester and universal testing machine. The hardness was measured by using Vickers hardness tester. For this purpose, the indenter was pressed with 200 gm of load in vertical direction on the sample for 10 s and then unloaded. The universal testing machine attached with a software was utilized for the measurement of strength and percentage elongation of the material. The deformation was recorded by the attached computer in the form of engineering stress–strain curves. The fractographs of solution treated and age-hardened Al-6061 samples were obtained by using the scanning electron microscope.

2. Results and Discussion.

2.1. X-ray Diffraction Study. X-ray diffraction (XRD) results of Al-6061 at different aging temperatures are shown in Fig. 1. The figure shows that the aging heat treatment of Al-6061 produces significant structural changes in the aluminum alloy. In the case of solution treated (ST) sample, only Al diffraction peaks corresponding to (111), (200) and (220) planes are found at 39.3°, 44.1°, and 64.5°, respectively (Ref. Card: 03-065-2869). The ST sample does not show any peak relating to Mg_2Si precipitates which indicates the complete dissolution of the solute atoms (Mg and Si) in the Al matrix to form supersaturated solid solution. aging of Al-6061 at different temperatures causes the formation of Mg_2Si precipitates in it as shown by the XRD results. The diffraction peaks of Mg_2Si were matched with the (Ref. Card: 01-075-0445), and these are consistent with the previous studies [10, 16]. Intensity of Mg_2Si peaks is much smaller than the intensity of Al peaks due to lower volume fraction of Mg_2Si phase as compared to the Al. When the Al-6061 samples are aged at 140°C, then two distinct peaks of Mg_2Si are observed. Furthermore, the Al (111) peak disappears and the intensities of Al (200) and Al (220) peaks are decreased. The lower intensities of Al suggest that the precipitation in the alloy suppresses the growth of grains and thus cause a decrease in the crystallinity of the material [17]. The Al (200) and Al (220) peaks are shifted at higher diffraction angles that

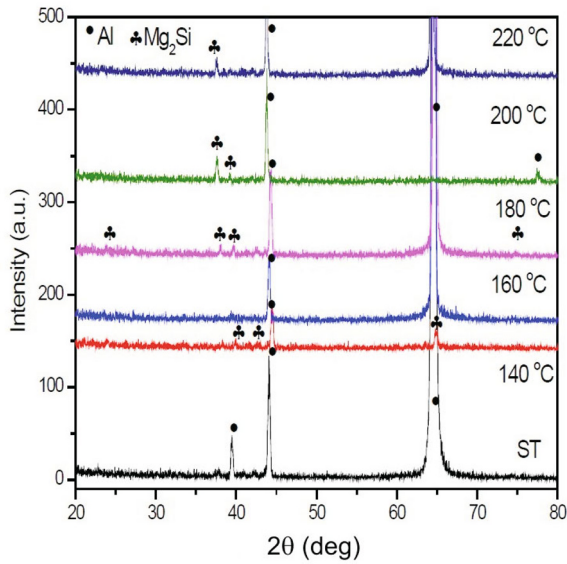


Fig. 1

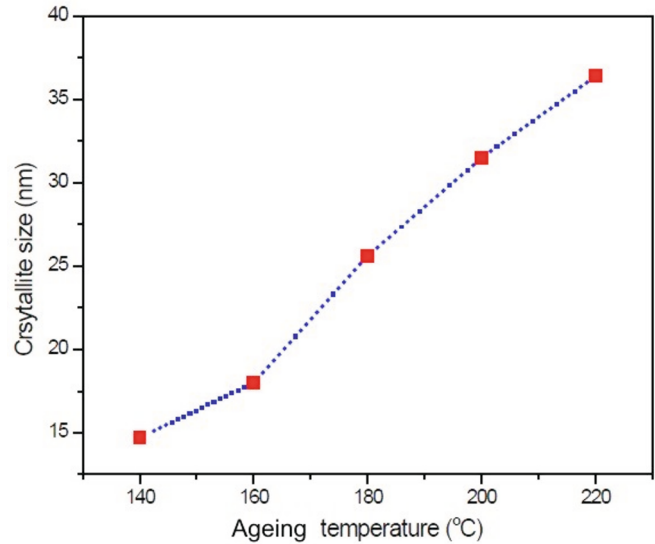


Fig. 2

Fig. 1. XRD patterns of Al-6061 at different aging temperatures.

Fig. 2. Changes in crystallite size with different aging temperatures.

indicates the rejection of Mg from the Al that reacts with Si to form $MgSi_2$ precipitates. Since, the Mg has larger radius than the Al, therefore, the higher angle peak shifting of the Al is observed. However, when the aging temperature increases to 160°C, this trend changes and the Al peaks are shifted to lower diffraction angles. Moreover, only a single distinct peak of $MgSi_2$ is observed, while no other peaks could be detected due to their amorphous nature. Increasing the aging temperature to 180 and 200°C, intensity of $MgSi_2$ peak increases. The Al (200) peak is shifted to higher angle at 180 and to lower angle at 200°C. This peak shifting signals towards the generation of compressive and tensile stresses during the aging process. At 220°C, only a single distinct peak of $MgSi_2$ is observed whereas no other peaks are visible due to their amorphous nature. This demonstrates that the Mg_2Si precipitates begin to dissolve in Al as the aging temperature increases above 200°C to form Al based supersaturated solution. The crystallite size of Al-6061 was calculated using the following relation [18, 19]:

$$D = \frac{k\lambda}{\beta \cos \theta},$$

where D is the crystallite size, λ is the wavelength, β is the full width at half maximum (FWHM) of the diffraction peak, and θ is the Bragg's angle. The changes in crystallite size of Mg_2Si precipitates with increase of aging temperature is shown in Fig. 2. The crystallite size increases with increase in the aging temperature. The increase in the crystal size of precipitates occurs due to the heat treatment of the material at higher aging temperature. During rapid cooling from the higher aging temperature till 200°C, the precipitates are not only formed in large amount, but these also grow in size. When the aging temperature increases to 220°C, then the amount of precipitation decreases, however, the crystallite size of $MgSi_2$ precipitates is further increased.

2.2. Surface Morphology. The scanning electron microscopy micrographs of ST and artificially aged Al-6061 samples are shown in Fig. 3. The ST sample's surface does not contain any significant feature. However, in the case aged samples, small dispersed particles are observed on the alloy surface. These particles are perhaps the Mg_2Si precipitates that are formed during the aging process and these are coherent with the Al matrix. These precipitates were formed during rapid cooling of the samples from the aging temperature [20, 21]. The solutes present in the Al-6061 such as silicon and magnesium reacted immediately to form Mg_2Si precipitates. As we see

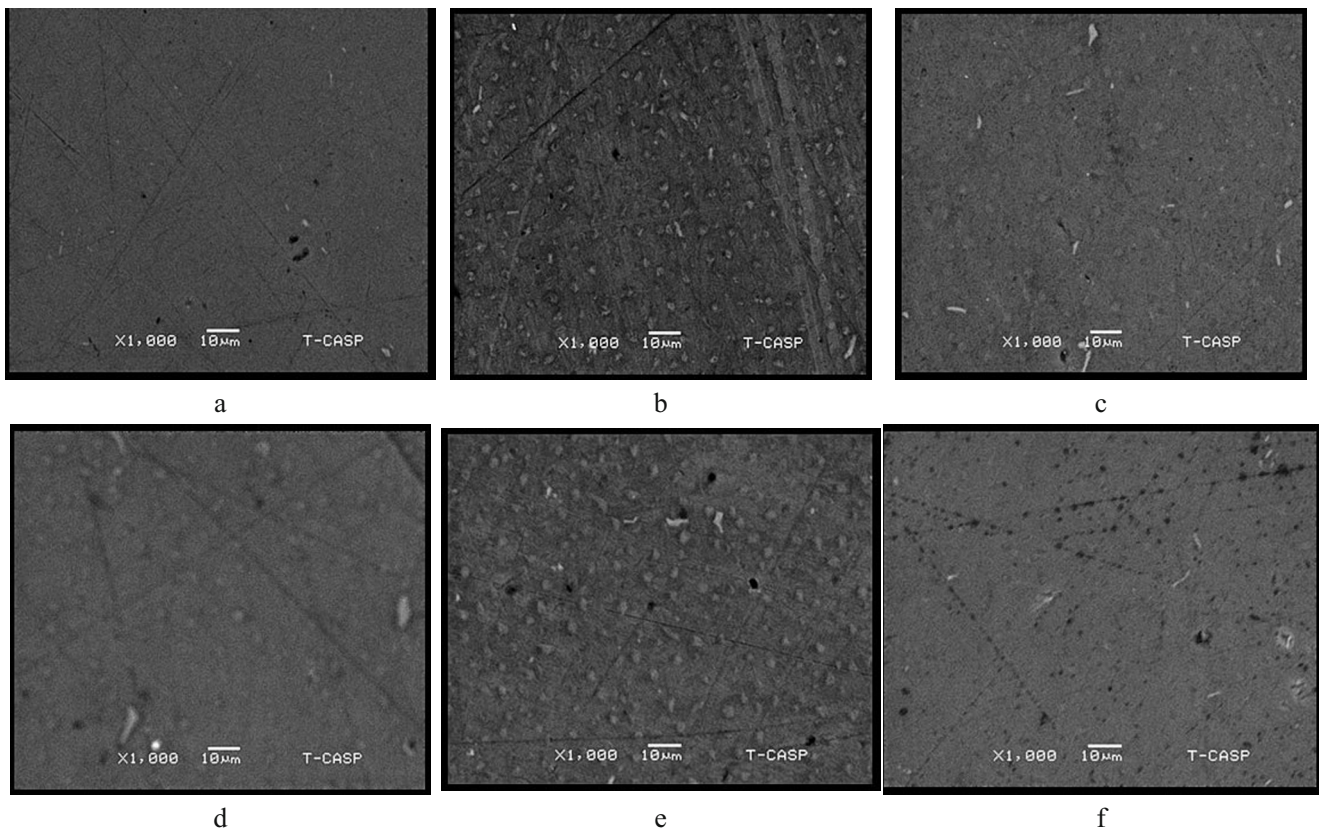


Fig. 3. SEM micrographs of Al-6061 alloy aged at different temperatures. Here and in Fig. 8: (a) solution treated; (b) 140°C; (c) 160°C; (d) 180°C; (e) 200°C; (f) 220°C.

from the figure that the precipitates size increases with increase in the aging temperature up to 200°C. The precipitates in the sample aged at 200°C are more prominent, coherent and uniform as compared to those that were aged at lower temperatures. In the case of sample aged at 220°C, the precipitates become incoherent and this signals towards a loss of the material's strength. As we see, the precipitate size increases with increase in the aging temperature. The surface morphology results are consistent with the XRD results both demonstrating an increase in the Mg_2Si precipitation in Al-6061 up to 200°C.

2.3. Mechanical Testing Results.

2.3.1. Hardness Measurements. The Vickers's hardness of Al-6061 at different aging temperatures are shown in Fig. 4. The figure shows an increase in hardness of the alloy with an increase in aging temperature to 200°C, however, the hardness decreases when the aging temperature reaches 220°C. When the aging temperature is increased from 140 to 160°C, the hardness increases from 72 to 85 HV. With a further increase in the temperature from 160 to 200°C, the hardness value is increased up to 92 HV. However, when the aging temperature reaches 220°C, the hardness is reduced. The hardness value at this temperature is 75 HV. This shows that the aging temperature of 200°C is more suitable as compared to other temperatures to achieve the optimum hardness value. The increase in Vickers hardness up to 200°C is linked to formation of Mg_2Si precipitates in Al-6061 alloy, hindering deformation under the applied force. As demonstrated in the SEM and XRD results, these precipitates are coherent with the alloy matrix and thus are the main source of increasing the material's hardness. However, when their size increases beyond a critical value, the precipitates' coarsening results in the formation of incoherent precipitates. These precipitates are not as effective against the dislocation movement as those of the coherent precipitates [22]. Therefore, a decrease in the hardness was observed with increase of the aging temperature to 220°C. The large Vickers hardness value obtained might be due to the pre-natural aging of the samples that resulted in the formation of stable precipitates that resist dislocation motion so the alloy is hardened.

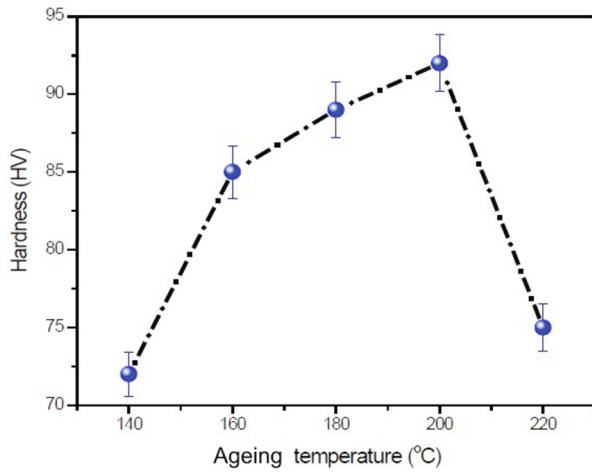


Fig. 4

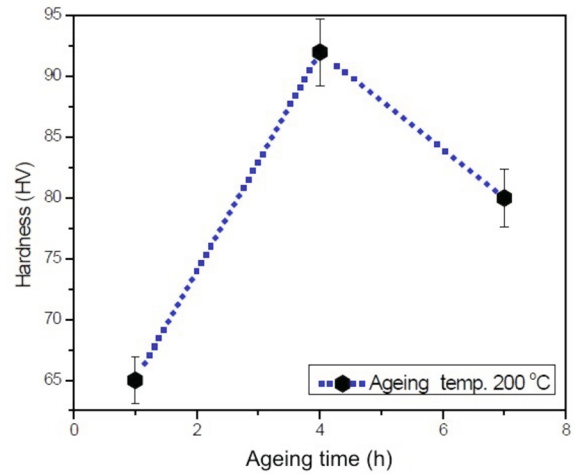


Fig. 5

Fig. 4. Hardness variation of Al-6061 alloy as function of ageing temperature.

Fig. 5. Hardness variation of Al-6061 alloy as function of ageing time.

The variation in hardness of Al-6061 alloy (aged at 200°C) with increase of aging time is shown in Fig. 5. The Vickers hardness increases with increase in the aging time from 1 to 4 h. However, when the aging time is increased to 7 h, the hardness is decreased. As observed from the temperature dependence hardness results in the previous section, it is through that the $MgSi_2$ precipitation/size increases with the aging time growth from 1 to 4 h. Therefore, the hardness increases due to the resistance offered by these precipitates to the indentation. As the aging time is increased to 7 h, there might be a decrease in the precipitation in Al-6061 aged alloy due to its over-aging. Consequently, the hardness decreases after aging the sample for 7 h.

2.3.2. Tensile Test Results. The stress–strain (SS) curves for the solution treated (ST) sample and the samples aged at different temperatures are shown in Fig. 6a. As we can see that there is a change in the yield stress (YS), ultimate tensile stress (UTS), and elongation of the material with changes in the aging temperature. The values of YS, UTS, and percentage elongation were obtained from the SS curves and these are plotted against the aging temperature as shown in Fig. 6b and c. The YS increases slowly when the Al-6061 sample is aged up to 160°C. However, when the aging temperature increases from 160 to 200°C, the YS rises sharply; the sample aging at 140°C increases the YS only by 11.3%, whereas the aging temperature rise to 200°C results in the increase in YS by 120%, as compared to the ST sample. At 220°C, the YS decreases by 15% from its value at 200°C. Similarly, the UTS also follows the similar trend, as shown by the YS. However, the changes in the UTS are relatively smaller than those of the YS. The UTS increases by 25% with aging temperature rise to 200°C. On the other hand, when aging temperature increases to 220°C, the UTS drops by 13.5% from its value at 200°C. The increase of YS and UTS with aging temperature rise to 200°C is due to hindrance offered by the Mg_2Si precipitates to the motion of glide dislocations [23, 24]. When the material is deformed, the produced dislocations move under the applied stress action. Meeting any obstacle in the material, dislocations stop, and a higher applied stress is required to continue their motion, increasing the material plasticity [25]. This study revealed that Mg_2Si precipitates formed during the aging heat treatment of the samples. The amount of Mg_2Si precipitation increased with the aging temperature rise to 200°C. These precipitates served as effective obstacles to the dislocation motion, and consequently the strength of Al-6061 was increased. When the aging temperature further increased to 220°C, the alloy strength dropped due to coarsening of the Mg_2Si precipitates beyond certain limit. This resulted in a loss of coherency between the Al matrix and the precipitates. These precipitates offered a weak resistance to the glide dislocations, deteriorating the Al-6061 alloy strength. The variation of percentage elongation with aging temperature is shown in Fig. 6c, which reveals insignificant changes in the percentage elongation with the aging temperature rise to 160°C, whereas above this temperature, the percentage elongation decreases. The decrease in percentage elongation above 160°C implies a less

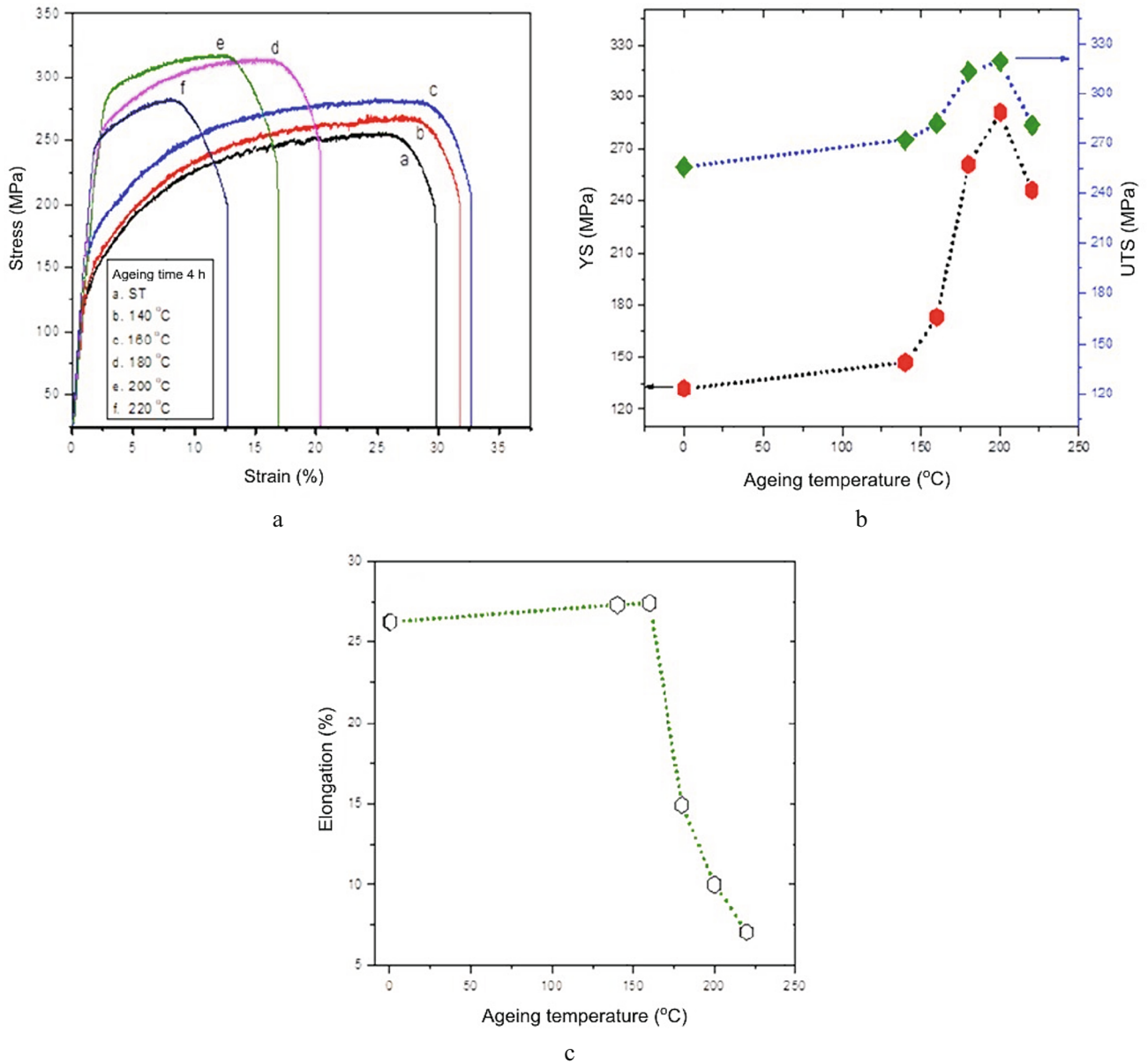


Fig. 6. Tensile testing results of Al-6061 aged at different temperatures.

pronounced the ductile behavior of the Al-6061 alloy. There is about a 73%-drop in the percentage elongation of Al-6061 upon its aging up to 220 °C. This shows that the material becomes brittle upon its artificial aging and this brittleness becomes more prominent at 220 °C. The insignificant change in the elongation of Al-6061 up to 160 °C indicates that the aging induced Mg_2Si precipitates are not much effective in resisting the dislocation motion. This is also supported by a small change in the YS and UTS of the alloy at this temperature. This might be due to their small size and the lesser amount of precipitation, causing minor changes in the stress and elongation of the material. However, as the precipitates size and amount increase, the decrease in the percentage elongation becomes more prominent due to their higher resistance to the moving dislocations.

The stress–strain curves of Al-6061 samples aged at 200 °C for 1, 4, and 7 h are shown in Fig. 7. As one can see from this figure that the YS and UTS increase rapidly as the aging time is increased to 4 h. In addition, the percentage elongation decreases after a 4 h aging time. However, when the aging time increases to 7 h, both YS and UTS are decreased. In addition, the percentage elongation also decreases. The increase of YS and UTS with increase

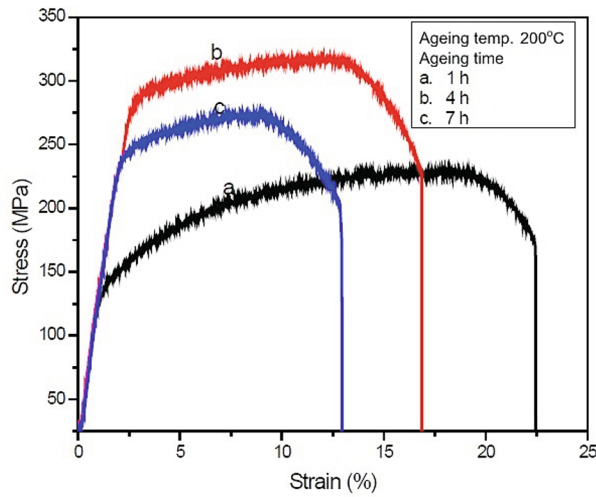


Fig. 7. Tensile testing results of Al-6061 aged for different durations.

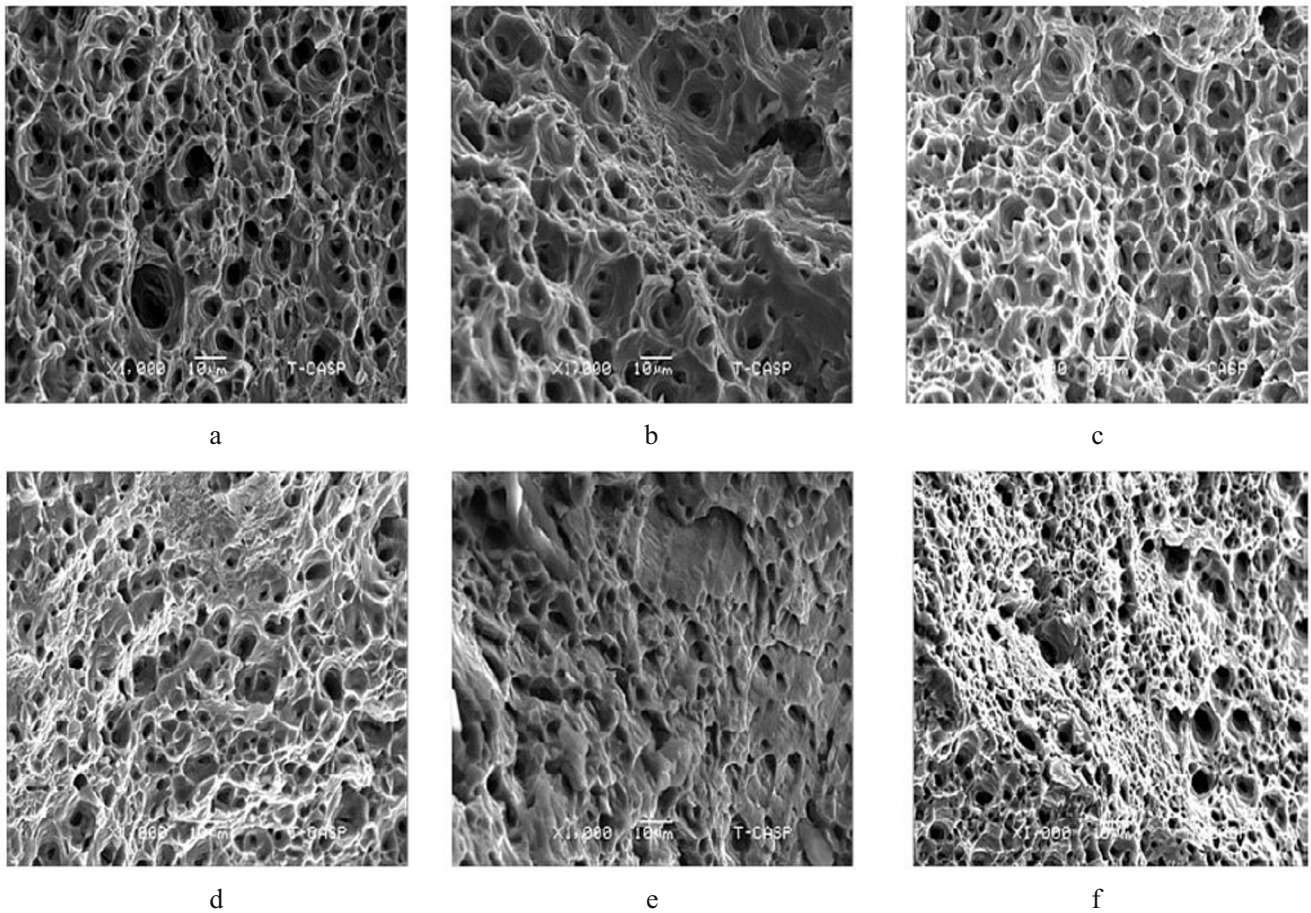


Fig. 8. Fractographs of Al-6061 aged at different temperatures.

of aging time to 4 h is due to the resistance offered by the Mg_2Si precipitates against the glide dislocations. Therefore, an increased stress is needed to continue the deformation and hence higher values of stresses are obtained after 4 h aging time. The higher value of stresses after 4 h aging time show higher amount of Mg_2Si precipitation in it. This precipitation decreases after 7 h of aging time and consequently the strength of the alloy is reduced. Due to

the resistance against dislocations motion by the precipitates, the plasticity of the alloy decreases. After 7 h of aging time, the decrease in the plasticity might be due localized defects inside the material. These results show that the optimum aging temperature and time for achieving the high strength is 200°C and 4 h, respectively.

2.3.3. Fractographs Results. The fractographs of Al-6061 alloy aged at different temperatures are shown in Fig. 8. The fractograph of solution treated (ST) sample shows dimples of different sizes, indicating a ductile cup and cone type fracture [26, 27]. After aging at 140°C, the dimples become small in size and their distribution becomes uniform over the whole surface. With increasing the aging temperature to 160°C, a variation in dimples shape and size is also noticed. The dimples size is relatively large as compared to that of the sample aged at 140°C, however, some very small size dimples are also present on the alloy surface. As the aging temperature increases to 180°C, the shape and size of the dimples change and these become relatively small in size as compared to those seen at lower temperatures. In addition, partial flatness of the sample's surface is also noticed along with the cracks that demonstrates a decrease in the ductility of the alloy. When the aging temperature is increased to 200°C, the dimples become very small and the surface flattens. The flatness of the surface is quite significant as compared with the sample aged at 180°C which signals towards a further decrease in the plasticity of the material. These results are consistent with the mechanical testing results as described above. At 220°C, the dimples size again reduces which is followed by the flatness of the surface, thus showing the brittle nature of the fracture.

Conclusions. Artificial aging of aluminum alloy 6061 causes the formation of Mg₂Si precipitates in it. With increase of the aging temperature, the crystallite size of Mg₂Si precipitates increases. The hardness and strength of the Al-6061 alloy increasing with increasing the aging temperature up to 200°C, however, at 220°C/4 h, the hardness is decreased. The Al-6061 hardness decreases as the aging time is increased to 7 h. The increase in the strength and hardness of the aluminum alloy-6061 is attributed to the resistance offered by Mg₂Si precipitates against the dislocation motion. The increased size of precipitates and the reduction of their amount decrease the hardness of the alloy aged at 220 and 200°C for 4 and 7 h, respectively. These results reveal that the optimum strength/hardness combination for Al-6061 alloy is provided by the its artificial aging at 200°C for 4 h.

REFERENCES

1. R. E. Sanders, Jr., "Technology innovation in aluminum products," *JOM*, **53**, 21–25 (2001).
2. I. Peter and M. Rosso, *Light Alloys — from Traditional to Innovative Technologies*, in: Z. Ahmad (Ed.), *New Trends in Alloy Development, Characterization and Application*, InTech, Rijeka, Croatia (2015), <https://dx.doi.org/10.5772/60769>.
3. X. Duan, Z. Mi, H. Jiang, et al., "Rapid bake-hardening response of Al–Mg–Si alloy during two-stage pre-aging heat treatment," *Mater. Res. Express*, **6**, No. 7, 076576 (2019).
4. W. S. Miller, L. Zhuang, J. Bottema, et al., "Recent development in aluminium alloys for the automotive industry," *Mat. Sci. Eng. A-Struct.*, **280**, 37–49 (2000).
5. S. M. Rajaa, H. A. Abdulhadi, K. S. Jabur, and G. R. Mohammad, "Aging time effects on the mechanical properties of Al 6061-T6 alloy," *Eng. Technol. Appl. Sci. Res.*, **8**, 3113–3115 (2018).
6. G. A. Edwards, K. Stiller, G. L. Dunlop, and M. J. Couper, "The precipitation sequence in Al–Mg–Si alloys," *Acta Mater.*, **46**, No. 11, 3893–3904 (1998).
7. O. Engler, C. D. Marioara, Y. Aruga, et al., "Effect of natural aging or pre-aging on the evolution of precipitate structure and strength during age hardening of Al–Mg–Si alloy AA 6016," *Mat. Sci. Eng. A-Struct.*, **759**, 520–529 (2019).
8. D. Maisonnette, M. Suery, D. Nelias, et al., "Effects of heat treatments on the microstructure and mechanical properties of a 6061 aluminium alloy," *Mat. Sci. Eng. A-Struct.*, **528**, No. 6, 2718–2724 (2011).
9. B. K. Barnwal, R. Raghvan, A. Tewari, and K. Narasimhan, "Effect of microstructure and texture on forming behaviour of AA-6061 aluminium alloy sheet," *Mat. Sci. Eng. A-Struct.*, **679**, 56–65 (2017).
10. S. Rajasekaran, N. K. Udayashankar, and J. Nayak, "T4 and T6 treatment of 6061 Al-15 vol.% SiC_p composite," *ISRN Mater. Sci.*, **2012**, Article ID 374719 (2012), <https://doi.org/10.5402/2012/374719>.

11. M. Murayama and K. Hono, "Pre-precipitate clusters and precipitation processes in Al-Mg-Si alloys," *Acta Mater.*, **47**, No. 5, 1537–1548 (1999).
12. D. Terada, Y. Kanda, Z. Horita, et al., "Mechanical properties and microstructure of 6061 aluminum alloy severely deformed by ARB process and subsequently aged at low temperatures," *IOP Conf. Ser.-Mat. Sci.*, **63**, 012088 (2014).
13. M. Mansourinejad and B. Mirzakhani, "Influence of sequence of cold working and aging treatment on mechanical behaviour of 6061 aluminum alloy," *T. Nonferr. Metal. Soc.*, **22**, No. 9, 2072–2079 (2012).
14. C. F. Tan and M. R. Said, "Effect of hardness test on precipitation hardening aluminium alloy 6061-T6," *Chiang Mai J. Sci.*, **36**, 276–286 (2009).
15. A. H. Naronikar, H. N. Akshay Jamadagnii, Amruthamshu Simha, and B. Saikiran, "Optimizing the heat treatment parameters of Al-6061 required for better formability," *Mater. Today-Proc.*, **5**, No. 11, 24240–24247 (2018).
16. Z. Liang, *Investigation on the Precipitation of Al-Mg-Si alloys with Different Heat Treatments*, Master Thesis, South China University of Technology (2009).
17. O. Engler, J. Hirsch, and K. Lücke, "Texture development in Al-1.8 wt% Cu depending on the precipitation state – II. Recrystallization textures," *Acta Metall. Mater.*, **43**, 121–138 (1995).
18. N. Afzal, M. Devarajan, and K. Ibrahim, "Effect of film thickness on the surface, structural and electrical properties of InAlN films prepared by reactive co-sputtering," *Mat. Sci. Semicon. Proc.*, **43**, 96–103 (2016).
19. R. Younas, N. Afzal, M. Rafique, et al., "Nickel ion implantation effects on DC magnetron sputtered ZnO film prepared on Si (100)," *Ceram. Int.*, **45**, No. 12, 15547–15555 (2019).
20. A. Cuniberti, A. Tolley, M. V. Castro Riglos, and R. Giovachini, "Influence of natural aging on the precipitation hardening of an AlMgSi alloy," *Mat. Sci. Eng. A-Struct.*, **527**, No. 20, 5307–5311 (2010).
21. M. E. Fine, "Precipitation hardening of aluminum alloys," *Metall. Mater. Trans. A*, **6**, No. 4, 625–630 (1975).
22. M. H. Jacobs, "The structure of the metastable precipitates formed during aging of an Al-Mg-Si alloy," *Philos. Mag. A*, **26**, 1–13 (1972).
23. F. Ozturk, A. Sisman, S. Toros, et al., "Influence of aging treatment on mechanical properties of 6061 aluminum alloy," *Mater. Design*, **31**, No. 2, 972–975 (2010).
24. P. Zhang, S. X. Li, and Z. F. Zhang, "General relationship between strength and hardness," *Mat. Sci. Eng. A-Struct.*, **529**, 62–73 (2011).
25. B.-L. Ou and C.-H. Shen, "Impact of pre-aging on the tensile and bending properties of AA 6061," *Scand. J. Metall.*, **34**, No. 6, 318–325 (2005).
26. V. K. Pandey, B. P. Patel, and S. Guruprasad, "Role of ceramic particulate reinforcements on mechanical properties and fracture behavior of aluminum-based composites," *Mat. Sci. Eng. A-Struct.*, **745**, 252–264 (2019).
27. A. Ghahremaninezhad and K. Ravi-Chandar, "Ductile failure behavior of polycrystalline Al 6061-T6 under shear dominant loading," *Int. J. Fracture*, **180**, 23–39 (2013).